Physics of Fluids

Dilute sodium dodecyl sulfate droplets impact on micropillar-arrayed non-wetting surfaces

Cite as: Phys. Fluids **33**, 107103 (2021); https://doi.org/10.1063/5.0064670
Submitted: 26 July 2021 • Accepted: 10 September 2021 • Published Online: 01 October 2021

Long-Zan Wang (王龙赞), **Xianfu Huang** (黄先富), **Quanzi Yuan** (袁泉子), **et al.**

Physics of Fluids ARTICLE scitation.org/journal/phf

Dilute sodium dodecyl sulfate droplets impact on micropillar-arrayed non-wetting surfaces

Cite as: Phys. Fluids 33, 107103 (2021); doi: 10.1063/5.0064670
Submitted: 26 July 2021 · Accepted: 10 September 2021 ·
Published Online: 1 October 2021

Long-Zan Wang (王龙赞),[1] Xianfu Huang (黄先富),[2,3] Quanzi Yuan (袁泉子),[2,3] Longquan Chen (陈龙泉),[4,5,a)] and Ying-Song Yu (余迎松)[1,a)]

AFFILIATIONS

[1]Department of Mechanics, School of Civil Engineering, Architecture and Environment, Hubei University of Technology, Wuhan 430068, People's Republic of China
[2]State Key Laboratory of Nonlinear Mechanics, Institute of Mechanics, Chinese Academy of Sciences, Beijing 100190, People's Republic of China
[3]School of Engineering Science, University of Chinese Academy of Sciences, Beijing 100049, People's Republic of China
[4]Yangtze Delta Region Institute (Huzhou), University of Electronic Science and Technology of China, Huzhou 313001, People's Republic of China
[5]School of Physics, University of Electronic Science and Technology of China, Chengdu 610054, People's Republic of China

[a)]Authors to whom correspondence should be addressed: lqchen@uestc.edu.cn and yuys@hbut.edu.cn

ABSTRACT

Impinging dilute sodium dodecyl sulfate (SDS) droplets on micropillar-arrayed polydimethylsiloxane surfaces were experimentally investigated. It was found that the behaviors of impinging droplets greatly depend on surface roughness and SDS concentration. Similar to pure water droplets, there exists a narrow range of dimensionless Weber number, We, for the complete rebound of impacting SDS droplets. The lower and upper limits of impact velocity were theoretically analyzed and compared with experimental data. The addition of SDS could greatly shorten the contact time of bouncing droplets. Besides, surface roughness has little influence on the maximum spreading factor while SDS concentration has an obvious influence and the maximum spreading factor nearly follows a scaling law of $We^{1/4}$.

I. INTRODUCTION

Droplet impacting on a solid surface is a ubiquitous phenomenon in nature and of great significance in agricultural and industrial fields.[1,2] And this phenomenon is found to be dependent on a lot of parameters such as the physical and chemical properties of droplets,[3–5] surface wettability,[6,7] surface roughness and shapes of the solid,[8–15] the tilt angle of the solid surfaces,[16–19] substrate elasticity,[20–23] substrate temperature,[24,25] the addition of particles into the liquid,[26] the application of external field,[27,28] and environmental conditions.[16,29,30] As a result, different behaviors of droplets including deposition, partial rebound, complete rebound, and splashing are easily observed. At certain conditions, jetting and bubbles[17,31–33] can be also observed during the impact process. Also, Mandre *et al.*[34] and Mani *et al.*[35] claimed that upon impact, a liquid droplet does not even contact the solid, and instead spreads on a very thin air film. Among the hot issues on this phenomenon, the rebound mechanism,[36–39] reducing the contact time[40–44] and maximum spreading factor[45–48] have attracted great attention of researchers.

Surfactants, which are usually composed of a polar hydrophilic head and one or more hydrophobic tails, can be used to reduce the surface tension of liquids. Because of the adsorption of surfactants at the liquid–vapor[49,50] and the solid–liquid interfaces[51,52] as well as the diffusion of surfactants inside droplets,[53] the impact dynamics of surfactant-laden droplets is quite different from that of pure liquid droplets. It has been experimentally demonstrated that the addition of surfactant will enhance the spreading of impacting droplets because of dynamic surface tension,[54–60] and the adsorption kinetics of surfactants has a great influence on droplet retraction.[56–58] Crooks *et al.*[61] concluded that the surfactant concentration has a great influence on the recoil behavior. When the concentration is less than the critical micelle concentration (CMC), the recoil behavior is controlled by droplet dynamics, otherwise it is governed by the demicellization. Besides the dynamic surface tension, the molecular weight and ionic nature of the surfactants as well as the non-wettability of the substrate also have great influence on droplet spreading.[62] Wang *et al.*[63] experimentally investigated the influence of surfactants on spontaneous

spreading of impacting droplets and found that surfactant properties have no influence on the wetting dynamics during the early inertia-dominated stage, but play a role in the later viscosity-dominated stage. On a hydrophobic surface, droplet rebound and droplet splashing can be inhibited by the addition of surfactants.[59,60,64] Luo *et al.*[65] observed uniform round droplet spreading and high-resolution inkjet printing patterns with the introduction of live-oligomeric surfactant into the liquid. However, to the best of our knowledge, there is no report of the influence of surfactants on impinging droplets onto substrates constructed with micro/nano-scale structures.

In this paper, impinging sodium dodecyl sulfate (SDS) droplets on micropillar-arrayed polydimethylsiloxane (PDMS) surface were investigated experimentally. And it was found that the behaviors of droplets greatly depend on SDS concentration and surface roughness. The addition of SDS can also greatly reduce the contact time of bouncing droplets. Moreover, surface roughness has little influence on the maximum spreading factor while SDS concentration has an obvious influence. The maximum spreading factor was found to nearly follow a scaling law of $We^{1/4}$.

II. MATERIALS AND METHODS

A. Substrate preparation

In this paper, three micropillar-arrayed PDMS surfaces with square lattices were prepared (the procedure to fabricate these surfaces can be found in Refs. 66 and 67). The diameter d and height h of each pillar were the same and they were both 20 μm. Pillar-to-pillar spacings w of the three surfaces were 5, 20, and 50 μm, respectively. And the corresponding solid fractions $\phi = \frac{\pi d^2}{4P^2}$ (where $P = d + w$) of the three surfaces were 0.50, 0.20, and 0.06, respectively.

B. SDS solution preparation

SDS with a purity of ≥99% purchased from Sigma-Aldrich was dissolved in de-ionized water and SDS solutions with concentrations of 0.1, 0.2, 0.5, and 1.0 CMC were obtained. The surface tension of an aqueous SDS solution will no longer be affected when its concentration is greater than 1 CMC (1 CMC is equal to 8.2 mM).[68,69] All solutions were prepared in glass and plastic containers which were cleaned in advance with acetone, ethanol, and de-ionized water successively. Each solution was used within a day from its preparation.

C. Measurement setup

The surface tension of SDS solutions was measured using a dynamic contact angle measuring devices and tensiometer (DCAT11, Dataphysics, Germany). The surface tensions of SDS solutions with concentrations of 0.1, 0.2, 0.5, and 1.0 CMC were measured to be respectively, 41.93 ± 0.03, 29.56 ± 0.03, 25.44 ± 0.03, and 30.58 ± 0.03 mN/m, indicating the surface tension of SDS solutions first decreases with increasing SDS concentration and then increases slightly with increase in SDS concentration, which is consistent with the results by Khalladi *et al.*[70] The wettability of dilute SDS droplets on micropillar-arrayed PDMS surfaces was studied with the help of a droplet shape analyzer (DSA30, Krüss, Germany). And the advancing and receding contact angles were measured by following the method suggested by Huhtamäki *et al.*[71] SDS droplets with an initial radius r_0 of 1.00–1.26 mm were generated from a NE30 needle and dropped freely from height ranging from 0.26 mm to 247.90 mm. The droplet impact was recorded using a high-speed camera (Nac Memrecam ACS-3, Japan) at 16000 fps. The ambient temperature and relative humidity were 21 ± 2 °C and 51 ± 4%, respectively. Each experiment was repeated at least three times to ensure reproductivity. Images were extracted from the videos and analyzed using the ImageJ software. Weber number (We) defined as $We = \rho V_0^2 r_0/\gamma_{lv}$ (where $\rho = 1000\,kg/m^3$, V_0 is impact velocity, and γ_{lv} is the surface tension of a SDS solution) was used to characterize the behavior of impacting droplets.

III. RESULTS AND DISCUSSION

A. Surface wettability

Table I lists the values of apparent contact angle θ_e, advancing contact angle θ_a, and receding contact angle θ_r of SDS droplets on micropillar-arrayed PDMS surfaces. On a planar PDMS surface, SDS droplets with concentrations of 0.1, 0.2, 0.5, and 1.0 CMC had apparent contact angles of 108° ± 2°, 105° ± 2°, 101° ± 2°, and 84° ± 2° (measured at temperature of 23 ± 2 °C and relative humidity of 42 ± 4%), respectively. If the wettability of SDS droplets on the micropillar-arrayed surfaces follows the Wenzel wetting model, then the apparent contact angles θ_W can be given as[72]

$$\cos\theta_W = r_f \cos\theta_Y, \tag{1}$$

where $r_f = 1 + \frac{\pi dh}{P^2}$ is the roughness factor, θ_Y is the Young's contact angle of a SDS droplet on a smooth PDMS surface and represented by the apparent contact angle of the droplet on a planar PDMS surface.

If the wettability follows the Cassie–Baxter wetting model, then the apparent contact angles θ_C can be expressed as[73]

$$\cos\theta_C = \phi\cos\theta_Y - 1 + \phi. \tag{2}$$

Substituting all the parameters into Eqs. (1) and (2), the corresponding values of Wenzel contact angle θ_W and Cassie–Baxter contact angle θ_C were obtained and listed in Table I. From Table I, it can be easily found that most of the apparent angles of SDS droplets on micropillar-pillared PDMS surfaces were greater than θ_W but less than θ_C, indicating that the droplets were at a mixed wetting state.[69,74] However, for the micropillar-arrayed PDMS surface with $\phi = 0.06$, the apparent contact angle of a 1.0 CMC SDS droplet was only slightly

TABLE I. Contact angles of water droplets on micropillar-arrayed PDMS surfaces.

ϕ	c_{SDS} (CMC)	θ_e	θ_W	θ_C	θ_a	θ_r
0.50	0.1	139° ± 2°	118°	153°	148° ± 2°	98° ± 2°
	0.2	136° ± 2°	113°	152°	148° ± 2°	93° ± 2°
	0.5	134° ± 2°	107°	151°	147° ± 2°	80° ± 2°
	1.0	121° ± 2°	81°	145°	130° ± 2°	76° ± 2°
0.20	0.1	141° ± 2°	123°	163°	150° ± 2°	111° ± 2°
	0.2	138° ± 2°	118°	162°	149° ± 2°	113° ± 2°
	0.5	137° ± 2°	110°	162°	149° ± 2°	74° ± 2°
	1.0	107° ± 2°	79°	159°	110° ± 2°	68° ± 2°
0.06	0.1	150° ± 2°	120°	170°	151° ± 2°	113° ± 2°
	0.2	150° ± 2°	115°	170°	151° ± 2°	67° ± 2°
	0.5	149° ± 2°	108°	170°	150° ± 2°	67° ± 2°
	1.0	88° ± 2°	80°	167°	90° ± 2°	59° ± 2°

greater than θ_C, which means that the droplet was nearly at the Wenzel wetting state.

No matter what the surface is, the apparent contact angle θ_e decreases with increasing SDS concentration. At SDS concentrations of 0.1, 0.2, and 0.5 CMC, there is little change in the advancing contact angle for the same micropillar-arrayed PDMS surface. However, the advancing contact angle decreases sharply when the concentration is 1.0 CMC, because increasing droplet volume will easily make the liquid contact the bottom of the surface under the action of gravity. For the case of determining the receding contact angle, the droplets may be able to reach the Wenzel wetting state because a much larger SDS droplet is generated at first and such a droplet may be easy to contact the bottom between micropillars under the action of gravity, especially for surfaces with sparser pillars.

B. Prediction of the limits of impact velocity of bouncing SDS droplets

Predicting the range of impact velocity for complete rebound or determining the lower and upper limits of impact velocity is of great significance. It has been widely accepted that the lower limit of impact velocity for complete rebound can be estimated by balancing the kinetic energy of the droplet just before hitting the surface $E_k = \frac{2}{3}\pi\rho R_0^3 V_0^2$ with the surface energy due to contact angle hysteresis $E_s = \pi r_{max}^2 \gamma_{lv}(\cos\theta_r - \cos\theta_a)$ (r_{max} is the maximum contact radius). Thus, the theoretical value of the lower limit of impact velocity, $V_{CL}^{theorec}$, can be given as[37]

$$V_{CL}^{theorec} = \sqrt{\frac{3\gamma_{lv} r_{max}^2(\cos\theta_r - \cos\theta_a)}{2\rho R_0^3}}. \quad (3)$$

Substituting the experimental data into Eq. (3), the values of $V_{CL}^{theorec}$ were obtained, as shown in Table II. It was found for most cases, the theoretical values $V_{CL}^{theorec}$ agreed well with the corresponding experimental data V_{CL}^{exp}. The great difference in the lower limit of impact velocity of a bouncing SDS droplet with SDS concentration of 0.1 CMC on the micropillar-arrayed PDMS surface with $\phi = 0.50$ might be attributed to viscous dissipation because the impact velocity was relatively high and viscous dissipation greatly depends on impact velocity.[43,75,76]

For the case of determining the upper limit of impact velocity for complete rebound, here we used our previous theoretical model taking into account partial penetration of liquid into the cavities between the micropillars. In this model, we assumed that the liquid partially penetrated into the cavities between micropillars but did not contact the bottom of the micropillar-arrayed surfaces. For simplicity, the liquid inside the cavities between the micropillars can be decomposed into two parts, as shown in Fig. 1. The height of the upper part and the meniscus height are h_1 and δ, respectively. Based on simple geometrical analysis, δ is found to be equal to $(\sqrt{2}P - d)^2/(8R)$.[38] Here, R is the curvature radius of the meniscus. Thus, the Laplace pressure can be given as[36,38]

$$p_L = 2\gamma_{lv}/R = 16\gamma_{lv}\delta/\left(\sqrt{2}P - d\right)^2. \quad (4)$$

The dynamic pressure can be expressed as[36,38]

$$p_d = 0.5\rho V_0^2. \quad (5)$$

In fact, there exists another pressure—water hammer pressure $p_h = \alpha\rho C V_0$,[9,68–70] where α is an empirical coefficient and $C = 1482$ m/s is the speed of sound in water. However, to date, there are still debates on the selection of the empirical coefficient.[8,77–79] Considering the interaction time of water hammer pressure is much less than those of Laplace pressure and the dynamic pressure, the water hammer pressure was neglected. Thus, the upper limit of impact velocity for complete rebound was estimated by balancing the Laplace pressure with the dynamic pressure. When $h_1 + \delta = h$, the droplet will contact the bottom of a micropillar-arrayed surface and no longer bounce off the surface due to the increase in solid–liquid adhesion. Therefore, the upper limit of impact velocity, V_{CU}, can be written as[39]

$$V_{CU} = \sqrt{\frac{32\gamma_{lv}(h - h_1)}{\rho\left(\sqrt{2}P - d\right)^2}} \quad (6)$$

Equation (6) can be used to predict the upper limit of impact velocity for complete rebound if h_1 is known. Unfortunately, it is difficult to get its value because liquid penetration during droplet impact is a ultra-fast process. However, if the experimental value of the upper limit of impact velocity V_{CU}^{exp} and other parameters were substituted into Eq. (6), h_1 can be derived and listed in Table II. Based on our experimental data of de-ionized water droplets[39] and aqueous SDS droplets impacting on micropillar-arrayed PDMS surfaces, $h_1 \approx 0.9h$ can be used to approximately predict the upper limit of impact velocity for complete rebound.

TABLE II. Analysis for the lower and upper limits of impact velocity of bouncing SDS droplets.

ϕ	c_{SDS} (CMC)	V_{CL}^{exp} (m/s)	$V_{CL}^{theorec}$ (m/s)	V_{CU}^{exp} (m/s)	h_1 (μm)
0.50	0.1	0.98	0.37	1.29	19.42
0.20	0.1	0.28	0.19	0.72	18.97
	0.2	0.31	0.16	0.79	18.20
	0.5	0.33	0.23	0.69	18.41
	1.0	0.31	0.24	0.55	19.16
0.06	0.1	0.17	0.15	0.38	18.66
	0.2	0.18	0.19	0.40	17.85
	0.5	0.22	0.19	0.22	19.24

C. Phase diagram of droplet impact

For SDS droplets hitting a micropillar-arrayed PDMS surface with $\phi = 0.50$, there existed a narrow range of Weber number for complete rebound when the initial SDS concentration is 0.1 CMC. When the SDS concentration increased to 0.2 CMC, droplets no longer bounced off the surface. The droplets were all at the state of deposition below a critical Weber number. Though deposition can be found at a wider range of We, it has different causes depending on the value of We. For example, when We = 5.5 [as shown in Fig. 2(a) (Multimedia view)], the kinetic energy of the droplet is much small and thus it cannot overcome the surface energy due to contact angle hysteresis. However, when We = 58.4 [as shown in Fig. 2(b)], the droplet has a much higher impact velocity and thus part of the liquid will penetrate into the cavities between the micropillars, resulting in a

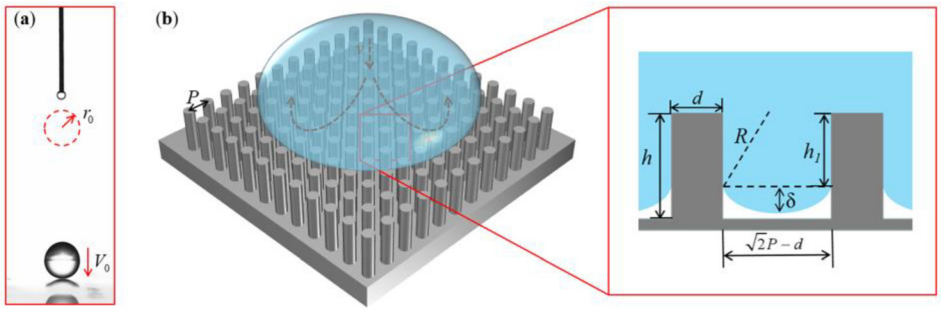

FIG. 1. Schematic for predicting the upper limit of impact velocity for complete rebound. (a) Schematic of an impacting droplet and (b) theoretical model.

stronger solid–liquid interaction, which acts as an extra barrier to prevent the droplet from leaving the surface during the retraction process. Moreover, when increasing We to a higher value, SDS droplets have a state of partial rebound.

For micropillar-arrayed PDMS surfaces with $\phi = 0.20$ or 0.06, the behavior of impinging SDS droplets was similar to that of pure water droplets.[39] First, there existed a range of We for complete rebound at SDS concentrations from 0.1 to 1.0 CMC on a micropillar-arrayed surface with $\phi = 0.20$, (it should be noted that droplet impact experiments with initial SDS concentration greater than 1.0 CMC have not been conducted) or from 0.1 to 0.5 CMC on a micropillar-arrayed surface with $\phi = 0.06$. Below the lower limit of We for complete rebound, all droplets were in a state of deposition. When the value of We was greater than its upper limit for complete rebound, droplets were in a state of partial rebound on the surface with $\phi = 0.20$ [as shown in Fig. 3(a) (Multimedia view)] while in a sticky state on the surface with $\phi = 0.06$ [as shown in Fig. 3(b)].

Figure 4 shows the snapshots of bouncing SDS droplets on a micropillar-arrayed PDMS surface with $\phi = 0.50$. It can be easily found that majority of the droplets could bounce off the surface while there was still a minor part of liquid left sticky on the surface. The reason might be attributed to the relatively stronger solid–liquid interaction because there was more wetted solid surface as compared to the other two surfaces and the impact velocities were relatively large, which makes liquid partial penetration into the cavities between micropillars more easy.

Figure 5 shows the snapshots of bouncing SDS droplets on a micropillar-arrayed PDMS surface with $\phi = 0.20$. For example, when We was 2.0, the droplets can completely bounce off the surface, as shown in Fig. 5(a). When We was 9.6, majority of the liquid would depart from the surface with a minor part of liquid left on the surface, as shown in Fig. 5(b). And the minor part would also rebound later. However, when We was 13.0 [Fig. 5(c)], though majority of the liquid bounced off the surface, the minor part would no longer bounce off the surface, indicating in this case some of the liquid had penetrated into the cavities between the micropillars, which made the solid–liquid interaction much stronger and thus the interaction hindered the rebound of the minor part.

Figures 6(a) and 6(b) show the snapshots of bouncing SDS droplets on a micropillar-arrayed PDMS surface with $\phi = 0.06$. It could be easily found that droplets could completely rebound without any remaining. Meanwhile, visible gaps were usually observed during the spreading and retraction processes [as shown in Figs. 6(a) and 6(b) (Multimedia view)], which is similar to the behavior of bouncing water droplets on the same surface.[39] However, when the value of We was only slightly greater than its upper limit for complete rebound [as shown

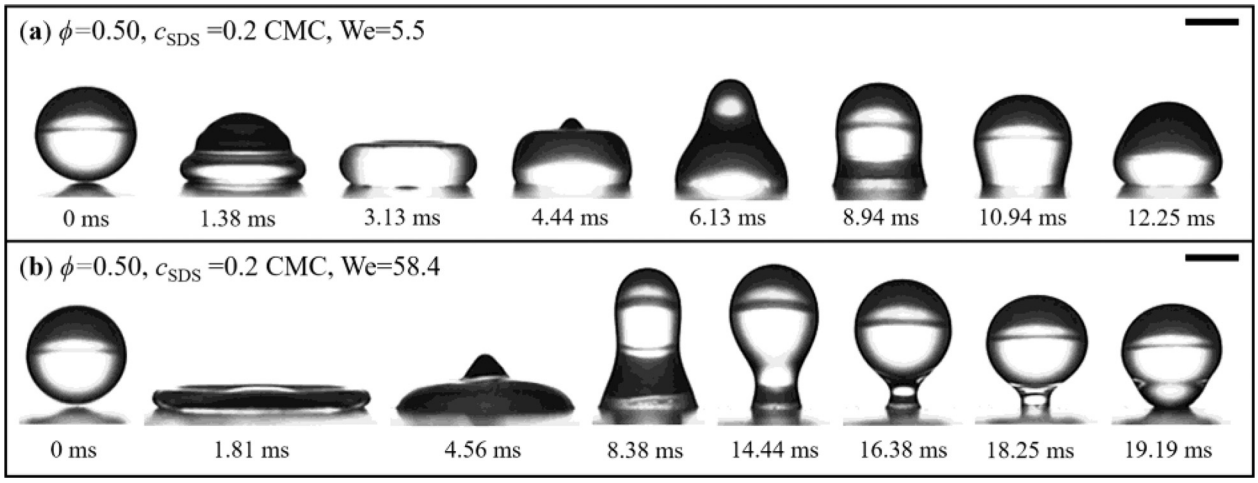

FIG. 2. Snapshots of 0.2 CMC SDS droplets impacting on a micropillar-arrayed PDMS surface with a solid fraction of $\phi = 0.50$ at different Weber numbers: (a) We = 5.5 and (b) We = 58.4. All inserted scale bars represent 1 mm. Multimedia views: https://doi.org/10.1063/5.0064670.1; https://doi.org/10.1063/5.0064670.2

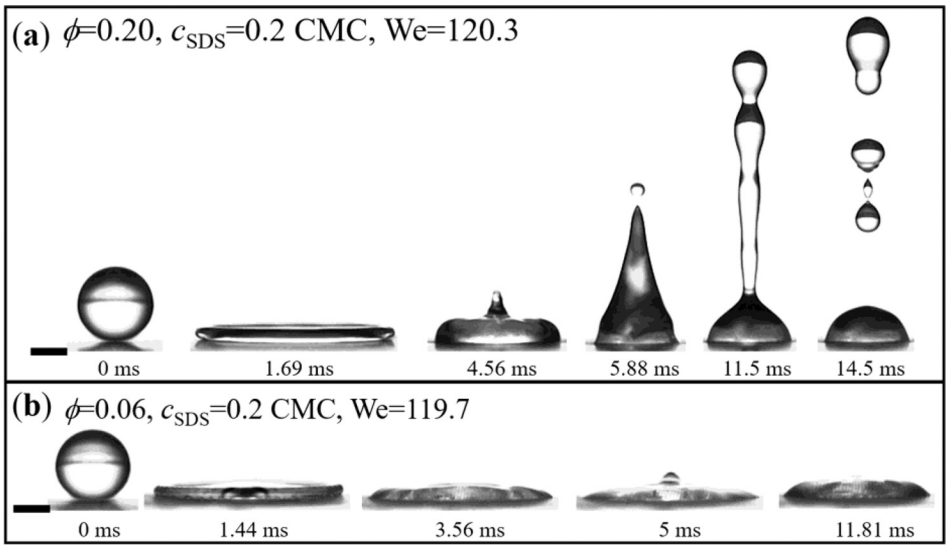

FIG. 3. Snapshots of SDS droplets impacting on micropillar-arrayed PDMS surfaces with different solid fraction at higher Weber number: (a) $\phi = 0.20$ and (b) $\phi = 0.06$. All inserted scale bars represent 1 mm. Multimedia views: https://doi.org/10.1063/5.0064670.3; https://doi.org/10.1063/5.0064670.4

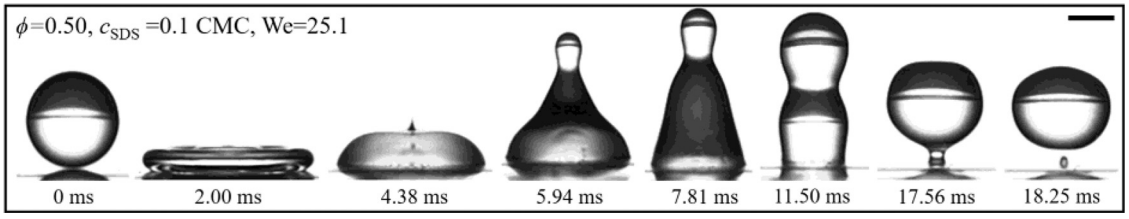

FIG. 4. Snapshots of bouncing 0.1 CMC SDS droplets on a micropillar-arrayed PDMS surface with $\phi = 0.50$ at We of 25.1. All inserted scale bars represent 1 mm.

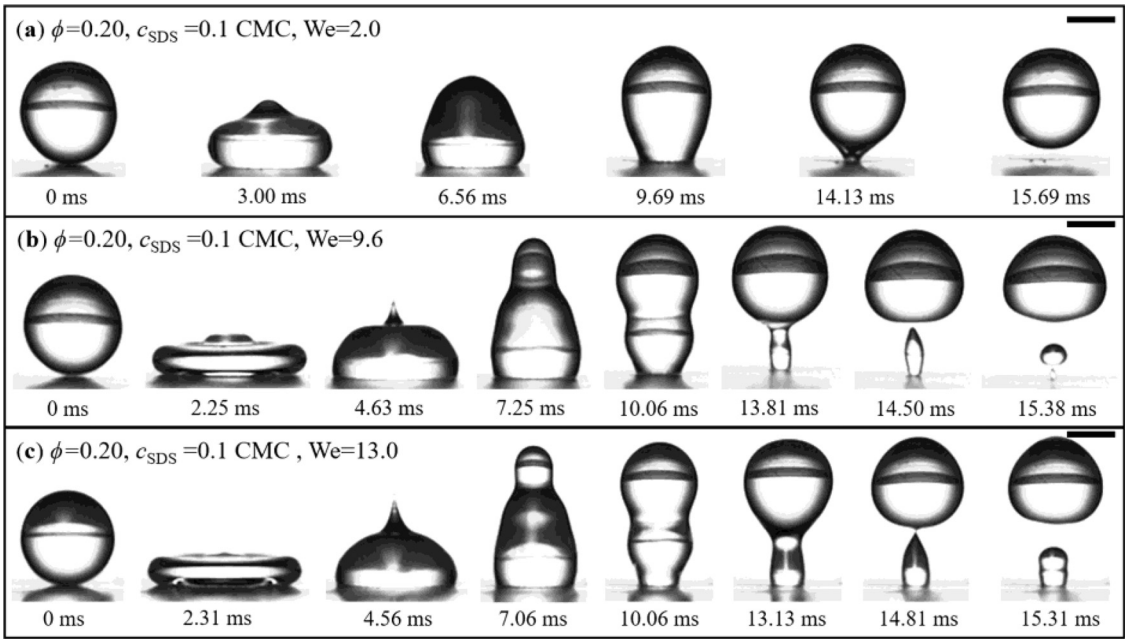

FIG. 5. Snapshots of bouncing 0.1 CMC SDS droplets on a micropillar-arrayed PDMS surface with $\phi = 0.20$ at different Weber numbers: (a) We = 2.0, (b) We = 9.6, and (c) We = 13.0. All inserted scale bars represent 1 mm.

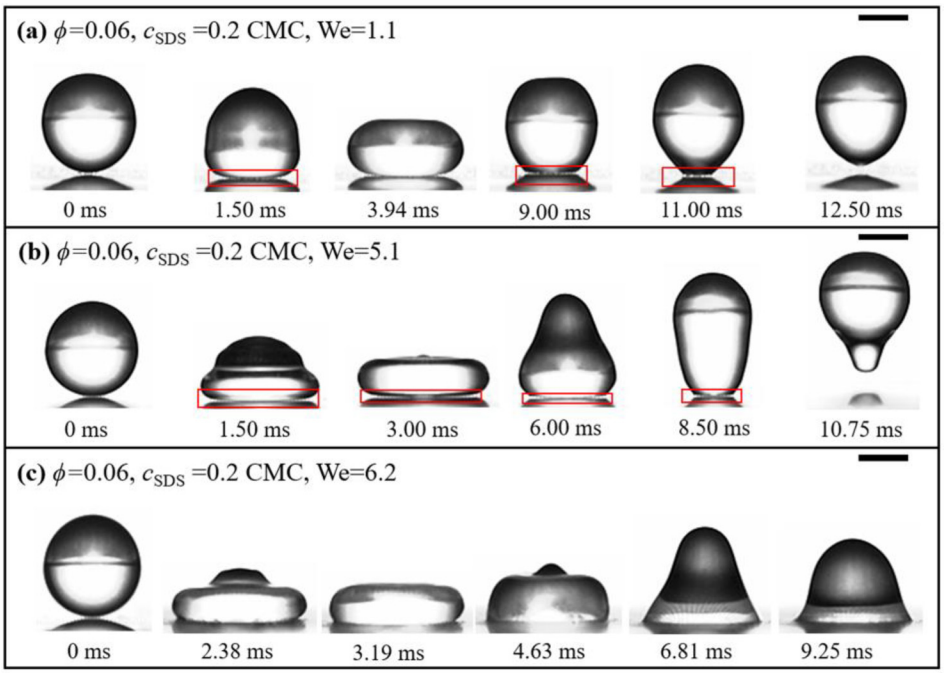

FIG. 6. Snapshots of 0.2 CMC SDS droplets impacting on a micropillar-arrayed PDMS surface with $\phi = 0.06$ at different Weber numbers: (a) We = 1.1, (b) We = 5.1, and (c) We = 6.2. All inserted scale bars represent 1 mm. Multimedia views: https://doi.org/10.1063/5.0064670.5; https://doi.org/10.1063/5.0064670.6

in Fig. 6(c) (Multimedia view)], no gaps were observed during the retraction process and thus the droplet was in a sticky state. Moreover, the contact angle of a bouncing droplet during the retraction process [as shown in Figs. 6(a) and 6(b)] was much greater than that of a non-bouncing droplet in the same process [as shown in Fig. 6(c)]. This indicates that there exists a transition from a Cassie–Baxter wetting state to a Wenzel wetting state. Because liquid completely occupies the space between the micropillars, there will be a great increase in the actual solid-liquid interfacial area, resulting in great increase in solid–liquid adhesion, which causes the droplet to be in a sticky state, as shown in Fig. 6(c).

Figure 7 summarizes the experimental phase diagram of the behavior of aqueous SDS droplets impacting on micropillar-arrayed PDMS surfaces [the outcome of pure water droplets impacting on the same micropillar-arrayed surfaces was extracted from Ref. 39 and added into Fig. 7. The behaviors of deposition, rebound, partial rebound, and sticky state are identical to those in Ref. 39 and the corresponding characteristic figures were omitted here]. It was found for most cases in our experiments that SDS droplets can bounce off micropillar-arrayed PDMS surfaces at a narrow range of We (as mentioned above, SDS droplets with concentration of 0.2 CMC cannot completely rebound from a micropillar-arrayed PDMS surface with $\phi = 0.50$). Below the lower limit of We for complete rebound, all droplets were in a state of deposition. Above the upper limit of We for complete rebound, SDS droplets could partially rebound from micropillar-arrayed surfaces with $\phi = 0.50$ and 0.20, while they were in a sticky state on a micropillar-arrayed surface with $\phi = 0.06$.

D. Contact time of bouncing droplets

Figure 8 summarizes the contact time of bouncing SDS droplets on micropillar-arrayed PDMS surfaces. To compare the influence of SDS concentration on the contact time, the characteristic contact time $\tau = 2.6\sqrt{\rho r_0^3/\gamma_{lv}}$[40] of bouncing droplets with SDS concentrations of 0.1, 0.2, 0.5, and 1.0 CMC was calculated and listed in Table III. For a micropillar-arrayed PDMS surface with $\phi = 0.50$, the values of contact time were all greater than that of pure water droplets and the corresponding characteristic value of the contact time. However, for micropillar-arrayed PDMS surfaces with $\phi = 0.20$ or 0.06, there was relatively small difference in the contact time as SDS was introduced to the liquid and the values of the contact time were all less than the corresponding characteristic values.

Moreover, the contact time t_c was decomposed into three parts, *viz.*, the spreading time t_s, the duration of pinned contact line stage t_p, and retraction time t_r. Table III lists the analysis of contact time. From Table III, it was found that the great reduction in the contact time of bouncing SDS droplets on micropillar-arrayed surfaces with $\phi = 0.20$ or 0.06 was mainly attributed to faster retraction. Besides, for the cases at fixed surface and SDS concentration, there was a great increase in retraction time as the impact velocity increased. The reason might be that droplets with higher impact velocity would more easily penetrate the cavities between micropillars.

E. Spreading and retraction

Figure 9 shows the influence of surface roughness on the maximum spreading factor $\beta_{max} = D_{max}/D_0$ (D_{max} and D_0 are the maximum spreading diameter and the initial spherical diameter of the droplets before hitting the surfaces, respectively) of SDS droplets impacting on micropillar-arrayed PDMS surfaces. It was found for a certain SDS concentration that surface roughness has no obvious influence on the maximum spreading factor.

Figure 10 shows the effect of SDS concentration on the maximum spreading factor. For a micropillar-arrayed PDMS surface with

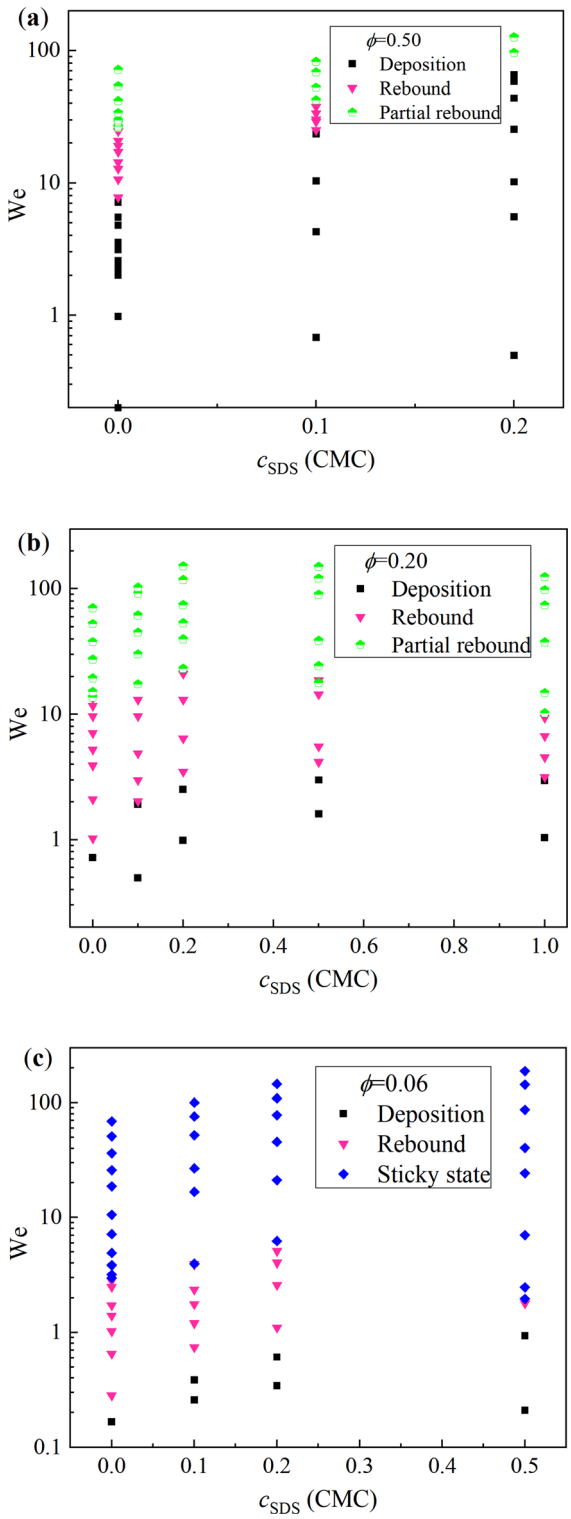

FIG. 7. Phase diagram of SDS droplets impacting on micropillar-arrayed PDMS surfaces with different solid fractions: (a) $\phi = 0.50$, (b) $\phi = 0.20$, and (c) $\phi = 0.06$. Multimedia views

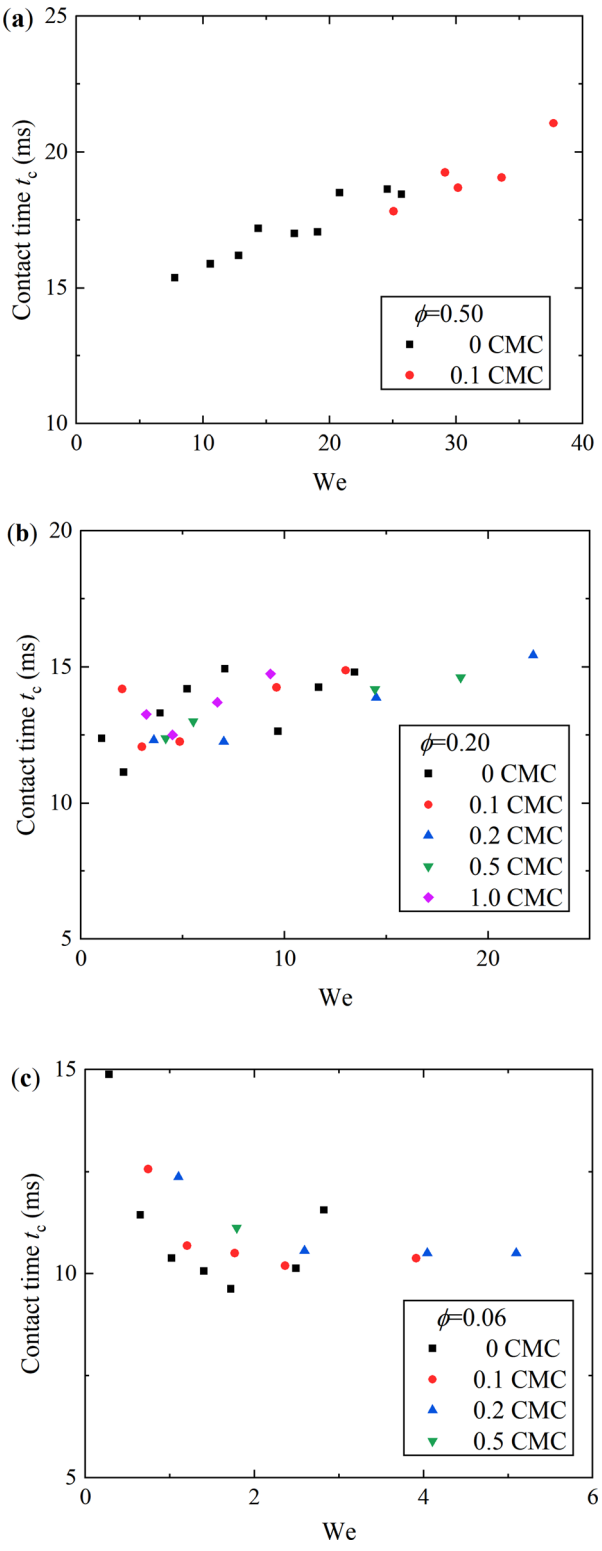

FIG. 8. Contact time of SDS droplets bouncing off micropillar-arrayed PDMS surfaces with different solid fractions: (a) $\phi = 0.50$, (b) $\phi = 0.20$, and (c) $\phi = 0.06$.

TABLE III. Time analysis for SDS droplets bouncing off micropillar-arrayed PDMS surfaces.

c_{SDS} (CMC)	ϕ	We	t_c (ms)	τ (ms)	t_s (ms)	t_p (ms)	t_r (ms)
0.1	0.50	25.1	17.81	17.10	2.06	1.56	14.19
	0.50	37.7	21.06	15.72	1.75	1.19	18.12
	0.20	3.0	12.06	16.48	2.81	3.44	5.81
	0.20	13.0	14.88	16.79	2.00	1.88	11.00
	0.06	0.7	12.56	17.10	3.69	3.81	5.06
	0.06	3.9	10.38	17.26	2.63	2.88	4.87
0.2	0.20	3.5	12.31	18.90	2.69	3.50	6.12
	0.20	21.1	15.45	18.54	2.13	1.88	11.44
	0.06	1.1	12.38	18.70	3.38	4.44	4.56
	0.06	5.1	10.50	17.98	2.50	2.19	5.81
0.5	0.20	4.2	12.37	18.07	2.81	4.00	5.56
	0.20	18.6	14.63	18.64	1.94	2.19	10.50
	0.06	1.8	11.13	17.86	2.94	4.13	4.06
1.0	0.20	3.2	13.26	16.31	3.44	3.19	6.63
	0.20	9.3	14.75	15.63	2.81	1.69	10.25

$\phi = 0.50$, the maximum spreading factor has a smaller value when increasing the SDS concentration [Fig. 10(a)] (in our experiments, only SDS droplets with SDS concentration of 0, 0.1, and 0.2 CMC have been conducted). For a micropillar-arrayed PDMS surface with $\phi = 0.20$ [Fig. 10(b)] or $\phi = 0.06$ [Fig. 10(c)], a similar phenomenon was found when increasing the SDS concentration in the range of 0–0.5 CMC. However, when the SDS concentration reached 1.0 CMC, the maximum spreading factor became larger as compared to an SDS concentration of 0.5 CMC at the same Weber number. The abnormal behavior may be attributed to partial penetration of the liquid into cavities between the micropillars. Moreover, the maximum spreading factors of impacting SDS droplets approximately follow a scaling law of $\beta_{max} \sim We^{1/4}$[47] (see Fig. 10).

At the moment of maximal deformation, the droplet is greatly flattened, which exhibits as a gravity puddle, as suggested by Clanet *et al.*[47] During the spreading of SDS droplets on these surfaces, the velocity of the droplets decreases from V_0 to 0 in a timescale of D_0/V_0, and thus the deceleration rate a scales as ${V_0}^2/D_0$, which is commonly about 50–200 times larger than the gravitational acceleration (in our experiments, $V_0 \sim 1$ m/s and $D_0 \sim 2$ mm). The thickness of the "puddle" under the effective "gravity field" scales as $\lambda = \sqrt{\gamma_{lv}/(\rho a)} = \sqrt{\gamma_{lv} D_0/(\rho {V_0}^2)}$. It couples with volume conservation ($\frac{\pi}{4} {D_{max}}^2 \lambda = \frac{\pi}{6} {D_0}^3$), leading to a maximum spreading factor as follows:[47]

$$\beta_{max} \sim We^{1/4}, \tag{7}$$

which is in good agreement with the experimental data, as shown in Fig. 10.

Figure 11 shows the normalized contact radius $r(t)/r_0$ (where $r(t)$ is the instantaneous contact radius) of SDS droplets impacting on micropillar-arrayed PDMS surfaces (the values of impact velocity were all about 1.5 m/s). In these cases, all droplets partially rebounded on the surfaces with $\phi = 0.50$ and 0.20 while they were in a state of sticky

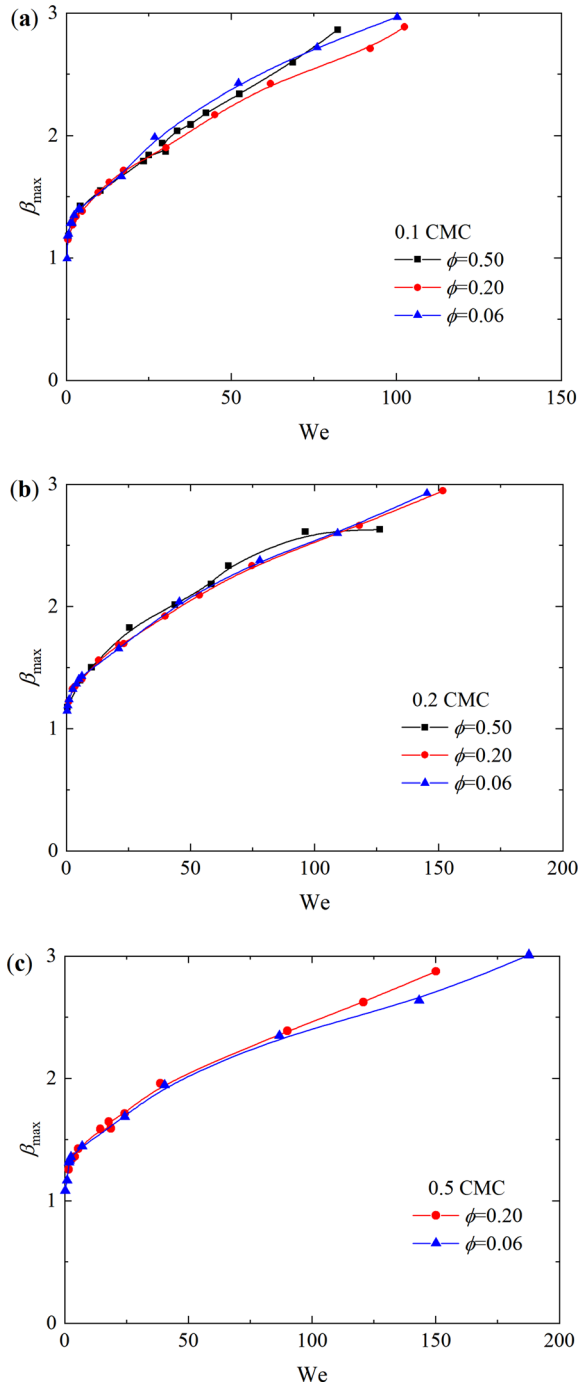

FIG. 9. Maximum spreading factor of impinging SDS droplets with different SDS concentrations: (a) 0.1, (b) 0.2, and (c) 0.5 CMC.

droplet on the surface with $\phi = 0.06$. From Fig. 11, we can easily find that there is no obvious difference in the spreading process. After the pinned contact line stage, all droplets would retract on the surface for a period and then the retraction would stop. On the surface with

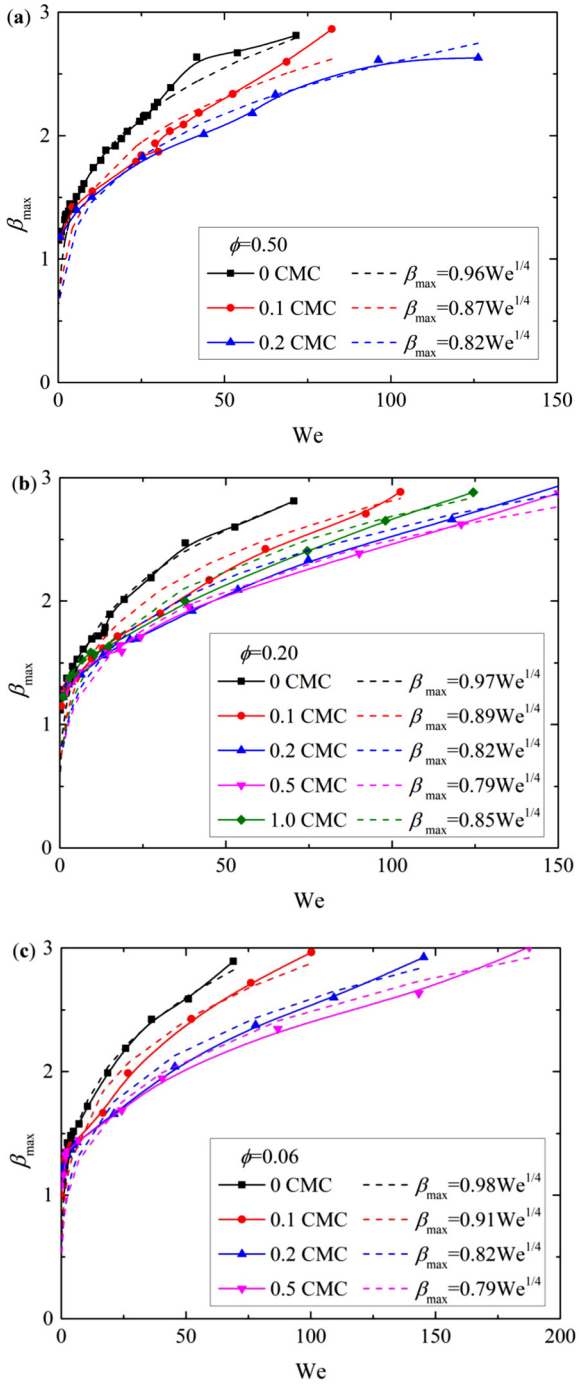

FIG. 10. Effect of SDS concentration on the maximum spreading factor of impacting SDS droplets on micropillar-arrayed PDMS surfaces with different solid fractions. (a) $\phi = 0.50$, (b) $\phi = 0.20$, and (c) $\phi = 0.06$.

$\phi = 0.50$, an SDS droplet with concentration of 0.2 CMC had a longer retraction time as compared to a pure water droplet and an SDS droplet with concentration of 0.1 CMC and the corresponding normalized contact radius had a lower value when the droplet stopped retraction.

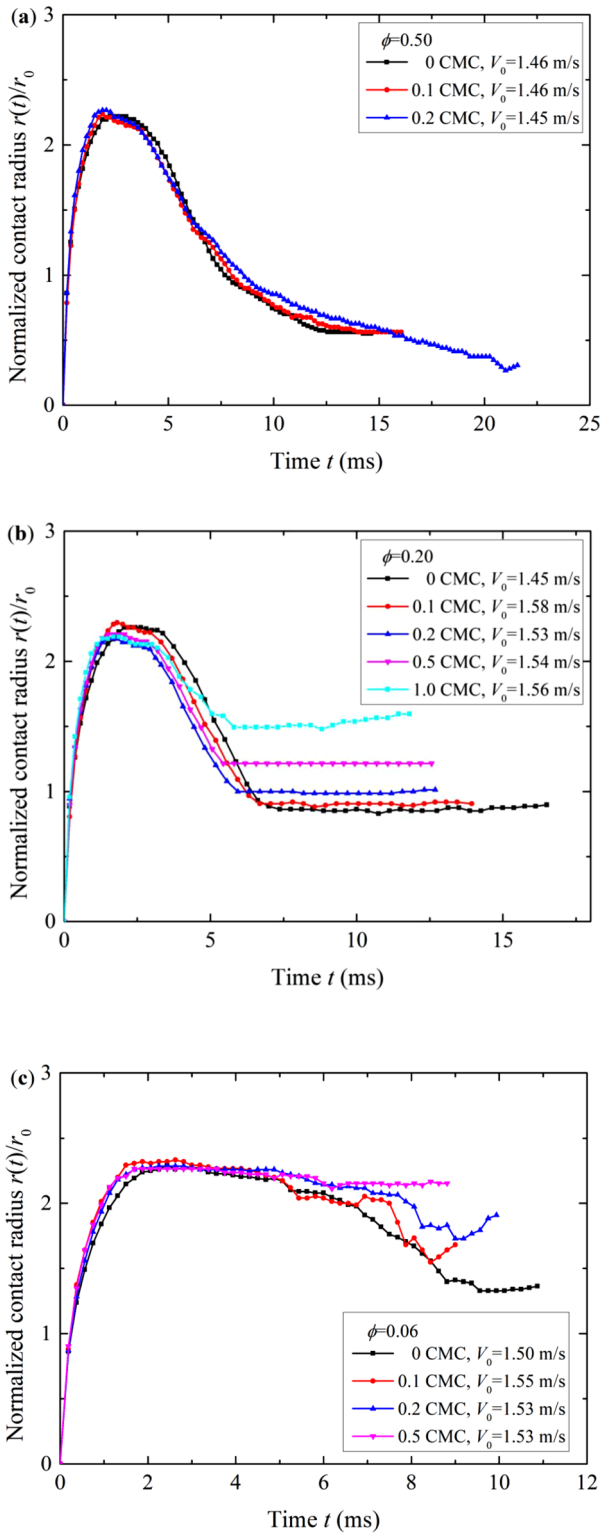

FIG. 11. Normalized contact radius of impacting SDS droplets on micropillar-arrayed PDMS surfaces. (a) $\phi = 0.50$, (b) $\phi = 0.20$, and (c) $\phi = 0.06$.

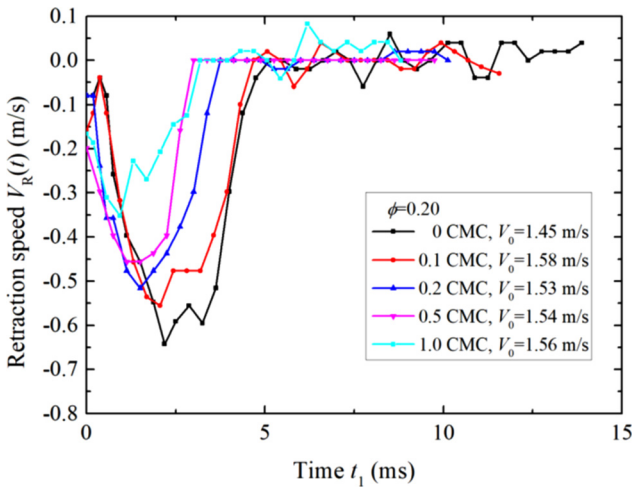

FIG. 12. Retraction speed of impacting SDS droplets on a micropillar-arrayed PDMS surface with $\phi = 0.20$.

However, for micropillar-arrayed surfaces with $\phi = 0.20$ and 0.06, with increasing SDS concentration, the normalized contact diameter has a larger value when the liquid no longer retracts. As an example, differentiating the instantaneous contact radius of SDS droplets on the surface with $\phi = 0.20$ [the data in Fig. 11(b)] with time, the corresponding retraction speed can be obtained (time t_1 was calculated from the end of the pinned contact line stage), as shown in Fig. 12. It was found that the maximum values of retraction speed V_R for SDS droplets with concentrations of 0, 0.1, 0.2, 0.5, and 1.0 CMC were 0.60, 0.56, 0.52, 0.46, and 0.35 m/s, respectively.

IV. CONCLUSIONS

Impinging dilute SDS droplets on micropillar-arrayed PDMS surfaces with different solid fractions were investigated experimentally. It was found that there existed a narrow range of Weber number for complete rebound of impacting droplets depending on the SDS concentration and surface roughness. The lower and upper limits of impact velocity for complete rebound of bouncing SDS droplets were theoretically analyzed and compared with experimental data. The contact time of bouncing droplets could be greatly reduced by adding SDS and adjusting the surface roughness. Similar to pure water droplets, maximum spreading factor of SDS droplets also nearly followed a scaling law of $We^{1/4}$. SDS concentration has an obvious influence on the maximum spreading factor while there is little influence of surface roughness on the maximum spreading factor. We envision that this work will broaden the application of surfactants and functional non-wetting surfaces.

ACKNOWLEDGMENTS

This work was jointly supported by the National Natural Science Foundation of China (Grant Nos. 11572114, 11772271, and 12072346); the PetroChina Innovation Foundation (Grant No. 2019D-5007-0102); and the Chinese Academy of Sciences Key Research Program of Frontier Sciences (Grant No. QYZDJ-SSW-JSC019).

AUTHOR DECLARATIONS

Conflicts of Interest

There are no conflicts of interest to declare.

DATA AVAILABILITY

The data supporting the findings of this study are available from the corresponding author upon reasonable request.

REFERENCES

[1]C. Josserand and S. T. Thoroddsen, "Drop impact on a solid surface," Ann. Rev. Fluid Mech. **48**, 365 (2016).
[2]D. Khojasteh, M. Kazerooni, S. Salarian, and R. Kamali, "Droplet impact on superhydrophobic surfaces: Review of recent developments," J. Ind. Eng. Chem. **42**, 1–14 (2016).
[3]B. Y. Zhao, X. Wang, K. Zhang, L. Q. Chen, and X. Deng, "Impact of viscous droplets on superamphiphobic surfaces," Langmuir **33**, 144 (2017).
[4]F. Gao, H. Yi, L. H. Qi, R. Qiao, and W. W. Deng, "Weakly charged droplets fundamentally change impact dynamics on flat surfaces," Soft Matter **15**, 5548 (2019).
[5]F. F. Yu, S. J. Lin, J. L. Yang, Y. Fan, D. H. Wang, L. Q. Chen, and X. Deng, "Prompting splash impact on superamphiphobic surfaces by imposing a viscous part," Adv. Sci. **7**, 1902687 (2020).
[6]S. J. Lin, B. Y. Zhao, S. Zou, J. W. Guo, Z. Wei, and L. Q. Chen, "Impact of viscous droplets on different wettable surfaces: impact phenomena, the maximum spreading factor, spreading time and post-impact oscillation," J. Colloid Interface Sci. **516**, 86–97 (2018).
[7]H. Almohammadi and A. Amirfazli, "Droplet impact: viscosity and wettability effects on splashing," J. Colloid Interface Sci. **553**, 22–30 (2019).
[8]L. Courbin, J. C. Bird, and H. A. Stone, "Splash and anti-splash: observation and design," Chaos **16**, 041102 (2006).
[9]L. K. Malla, N. D. Patil, R. Bhardwaj, and A. Neild, "Droplet bouncing and breakup during impact on a microgrooved surface," Langmuir **33**, 9620 (2017).
[10]C. J. Lv, P. F. Hao, X. W. Zhang, and F. He, "Drop impact upon superhydrophobic surfaces with regular and hierarchical roughness," Appl. Phys. Lett. **108**, 141602 (2016).
[11]Y. H. Liu, M. Andrew, J. Li, J. M. Yeomans, and Z. K. Wang, "Symmetry breaking in drop bouncing on curved surfaces," Nat. Commun. **6**, 10034 (2015).
[12]X. P. Huang, X. W. Dong, J. Li, and J. L. Liu, "Droplet impact induced large deflection of a cantilever," Phys. Fluids **31**, 062106 (2019).
[13]H. X. Zhang, X. Yi, Y. X. Du, R. Zhang, X. W. Zhang, F. He, F. L. Niu, and P. F. Hao, "Dynamic behavior of water drops impacting on cylindrical superhydrophobic surfaces," Phys. Fluids **31**, 032104 (2019).
[14]S. Y. Ding, X. Liu, X. M. Wu, and X. Zhang, "Droplet breakup and rebound during impact on small cylindrical superhydrophobic targets," Phys. Fluids **32**, 102106 (2020).
[15]F. Yeganehdoust, R. Attarzadeh, A. Dolatabadi, and I. Karimfazli, "A comparison of bioinspired slippery and superhydrophobic surfaces: micro-droplet impact," Phys. Fluids **33**, 022105 (2021).
[16]J. G. Hao, J. Lu, L. N. Lee, Z. H. Wu, G. K. Hu, and J. M. Floryan, "Droplet splashing on an inclined surface," Phys. Rev. Lett. **122**, 054501 (2019).
[17]J. W. Guo, S. Zou, S. J. Lin, B. Y. Zhao, X. Deng, and L. Q. Chen, "Oblique droplet impact on superhydrophobic surfaces: Jets and bubbles," Phys. Fluids **32**, 122112 (2020).
[18]J. Y. Liu, J. L. Song, G. S. Wang, F. Z. Chen, S. Liu, X. L. Yang, J. Sun, H. X. Zheng, L. Huang, Z. J. Jin, and X. Liu, "Maskless hydrophilic patterning of the superhydrophobic aluminum surface by an atomic pressure microplasma jet for water adhesion controlling," ACS Appl. Mater. Interfaces **10**, 7497 (2018).
[19]Y. J. Wang, A. E. Bouhai, S. J. Lyu, L. Yu, Y. Hao, Z. G. Zuo, S. H. Liu, and C. Sun, "Leidenfrost drop impact on inclined superheated substrates," Phys. Fluids **32**, 112113 (2020).
[20]R. E. Pepper, L. Courbin, and H. A. Stone, "Splashing on elastic membranes: The importance of early-time dynamics," Phys. Fluids **20**, 082103 (2008).

[21]A. Alizadeh, V. Bahadur, W. Shang, Y. Zhu, D. Buckley, A. Dhinojwala, and M. Sohal, "Influence of substrate elasticity on droplet impact dynamics," Langmuir **29**, 4520 (2013).
[22]L. Q. Chen, E. Bonaccurso, P. Deng, and H. Zhang, "Droplet impact on soft viscoelastic surfaces," Phys. Rev. E **94**, 063117 (2016).
[23]C. J. Howland, A. Antkowiak, J. R. Castrejón-Pita, S. D. Howison, J. M. Oliver, R. W. Style, and A. A. Castrejón-Pita, "It's harder to splash on soft solids," Phys. Rev. Lett. **117**, 184502 (2016).
[24]H. J. J. Staat, T. Tran, B. Geerdink, G. Riboux, C. Sun, J. M. Gordillo, and D. Lohse, "Phase diagram for droplet impact on superheated surfaces," J. Fluid Mech. **779**, R3 (2015).
[25]B. Li, S. J. Lin, Y. L. Wang, Q. Z. Yuan, S. W. Joo, and L. Q. Chen, "Promoting rebound of impinging viscoelastic droplets on heated superhydrophobic surfaces," New J. Phys. **22**, 123001 (2020).
[26]V. Grishaev, C. S. Iorio, F. Dubois, and A. Amirfazli, "Impact of particle-laden drops: particle distribution on the substrate," J. Colloid Interface Sci. **490**, 108 (2017).
[27]A. Ahmed, A. J. Qureshi, B. A. Fleck, and P. R. Waghmare, "Effects of magnetic field on the spreading dynamics of an impinging ferrofluid droplet," J. Colloid Interface Sci. **532**, 309 (2018).
[28]J. G. Zhen, Y. Cheng, Y. Z. Huang, S. X. Wang, L. Y. Liu, and G. Chen, "Drop impacting on a surface with adjustable wettability based on the dielectrowetting effect," Phys. Fluids **32**, 097108 (2020).
[29]L. Xu, W. W. Zhang, and S. R. Nagel, "Drop splashing on a dry smooth surface," Phys. Rev. Lett. **94**, 184505 (2005).
[30]E. Q. Li, K. R. Langley, Y. S. Tian, P. D. Hicks, and S. T. Thoroddsen, "Double contact during drop impact on a solid under reduced air pressure," Phys. Rev. Lett. **119**, 214502 (2017).
[31]Y. Renardy, S. Popinet, L. Duchemin, M. Renardy, S. Zaleski, C. Josserand, M. A. Drumright-Clarke, D. Richard, C. Clanet, and D. Quéré, "Pyramidal and toroidal water drops after impact on a solid surface," J. Fluid Mech. **484**, 69–83 (2003).
[32]D. Bartolo, C. Josserand, and D. Bonn, "Singular jets and bubbles in drop impact," Phys. Rev. Lett. **96**, 124501 (2006).
[33]S. J. Lin, D. H. Wang, L. J. Zhang, Y. K. Jin, Z. G. Li, E. Bonaccurso, Z. L. You, X. Deng, and L. Q. Chen, "Macrodrop-impact-mediated fluid microdispensing," Adv. Sci. **8**, 2101331 (2021).
[34]S. Mandre, M. Mani, and M. P. Brenner, "Precursors to splashing of liquid droplets on a solid surface," Phys. Rev. Lett. **102**, 134502 (2009).
[35]M. Mani, S. Mandre, and M. P. Brenner, "Events before droplet splashing on a solid surface," J. Fluid Mech. **647**, 163 (2010).
[36]D. Bartolo, F. Bouamrirene, É. Verneuil, A. Buguin, P. Silberzan, and S. Moulinet, "Bouncing or sticky droplets: Impalement transitions on superhydrophobic micropatterned surfaces," Europhys. Lett. **74**, 299 (2006).
[37]M. Reyssat, A. Pépin, F. Marty, Y. Chen, and D. Quéré, "Bouncing transitions on microtextured materials," Europhys. Lett. **74**, 306 (2006).
[38]Y. C. Jung and B. Bhushan, "Dynamic effects of bouncing water droplets on superhydrophobic surfaces," Langmuir **24**, 6262 (2008).
[39]L. Z. Wang, A. Zhou, J. Z. Zhou, L. Q. Chen, and Y. S. Yu, "Droplet impact on pillar-arrayed non-wetting surfaces," Soft Matter **17**, 5932 (2021).
[40]D. Richard, C. Clanet, and D. Quéré, "Contact time of a bouncing drop," Nature **417**, 811 (2002).
[41]J. C. Bird, R. Dhiman, H. M. Kwon, and K. K. Varanasi, "Reducing the contact time of a bouncing drop," Nature **503**, 385 (2013).
[42]Y. H. Liu, L. Moevius, X. P. Xu, T. Z. Qian, J. M. Yeomans, and Z. K. Wang, "Pancake bouncing on superhydrophobic surfaces," Nat. Phys. **10**, 515 (2014).
[43]H. P. Wu, K. P. Jiang, Z. X. Xu, S. H. Yu, X. Peng, Z. Zhang, H. Bai, A. P. Liu, and G. Z. Chai, "Theoretical and experimental studies on the controllable pancake bouncing behavior of droplets," Langmuir **35**, 17000 (2019).
[44]H. Y. Liu, F. Q. Chu, J. Zhang, and D. S. Wen, "Nanodroplets impact on surfaces decorated with ridges," Phys. Rev. Fluids **5**, 074201 (2020).
[45]M. Rein, "Phenomena of liquid drop impact on solid and liquid surfaces," Fluid. Dyn. Res. **12**, 61 (1993).
[46]T. Bennett and D. Poulikakos, "Splat-quench solidification: estimating the maximum spreading of a droplet impacting on a solid surface," J. Mater. Sci. **28**, 963 (1993).
[47]C. Clanet, C. Béguin, D. Richard, and D. Quéré, "Maximal deformation of an impacting drop," J. Fluid Mech. **517**, 199 (2004).
[48]H. M. Huang and X. P. Chen, "Energetic analysis of drop's maximum spreading on solid surface with low impact speed," Phys. Fluids **30**, 022106 (2018).
[49]J. Eastoe, J. S. Dalton, P. G. A. Rogueda, E. R. Crooks, A. R. Pitt, and E. A. Simister, "Dynamic surface tensions of nonionic surfactant solutions," J. Colloid Interface Sci. **188**, 423 (1997).
[50]A. Marin, R. Liepelt, M. Rossi, and C. J. Kähler, "Surfactant-driven flow transitions in evaporating droplets," Soft Matter **12**, 1593 (2016).
[51]S. Manne and H. E. Gaub, "Molecular organization of surfactants at solid-liquid interfaces," Science **270**, 1480 (1995).
[52]M. Duan, H. Wang, S. W. Fang, and Y. Liang, "Real-time monitoring the adsorption of sodium dodecyl sulfate on a hydrophobic surface using dual polarization interferometry," J. Colloid Interface Sci. **417**, 285 (2014).
[53]P. G. Nilsson and B. Lindman, "Mixed micelles of nonionic and ionic surfactants. A nuclear magnetic resonance self-diffusion and proton relaxation study," J. Phys. Chem. A **88**, 5391 (1984).
[54]X. G. Zhang and O. A. Basaran, "Dynamic surface tension effects in impact of a drop with a solid surface," J. Colloid Interface Sci. **187**, 166 (1997).
[55]M. Pasandideh-Fard, Y. M. Qiao, S. Chandra, and J. Mostaghimi, "Capillary effects during droplet impact on a solid surface," Phys. Fluids **8**, 650 (1996).
[56]N. Mourougou-Candoni, B. Prunet-Foch, F. Legay, M. Vignes-Adler, and K. Wong, "Influence of dynamic surface tension on the spreading of surfactant solution droplets impacting onto a low-surface-energy solid substrate," J. Colloid Interface Sci. **192**, 129 (1997).
[57]N. Mourougou-Candoni, B. Prunet-Foch, F. Legay, and M. Vignes-Adler, "Retraction phenomena of surfactant solution drops upon impact on a solid substrate of low surface energy," Langmuir **15**, 6563 (1999).
[58]M. Aytouna, D. Bartolo, G. Wegdam, D. Bonn, and S. Rafaï, "Impact dynamics of surfactant laden drops: dynamic surface tension effects," Exp. Fluids **48**, 49–57 (2010).
[59]K. P. Gatne, M. A. Jog, and R. M. Manglik, "Surfactant-induced modification of low Weber number droplet impact dynamics," Langmuir **25**, 8122 (2009).
[60]Z. L. Li, Y. Ma, K. F. Zhao, C. H. Zhang, Y. X. Gao, and F. P. Du, "Regulating droplet impact and wetting behaviors on hydrophobic weed leaves by a double-chain cationic surfactant," ACS Sustainable Chem. Eng. **9**, 2891 (2021).
[61]R. Crooks, J. Cooper-Whitez, and D. V. Boger, "The role of dynamic surface tension and elasticity on the dynamics of drop impact," Chem. Eng. Sci. **56**, 5575 (2001).
[62]A. Esmaeili, N. Mir, and R. Mohammadi, "Further step toward a comprehensive understanding of the effect of surfactant additions on altering the impact dynamics of water droplets," Langmuir **37**, 841 (2021).
[63]X. Wang, L. Q. Chen, and E. Bonaccurso, "Comparison of spontaneous wetting and drop impact dynamics of aqueous surfactant solutions on hydrophobic polypropylene surfaces: Scaling of the contact radius," Colloid Polym. Sci. **293**, 257 (2015).
[64]M. R. Song, J. Ju, S. Q. Luo, Y. C. Han, Z. C. Dong, Y. L. Wang, Z. Gu, L. J. Zhang, R. R. Hao, and L. Jiang, "Controlling liquid splash on superhydrophobic surfaces by a vesicle surfactant," Sci. Adv. **3**, e1602188 (2017).
[65]S. Q. Luo, Z. D. Chen, Z. C. Dong, Y. X. Fan, Y. Chen, B. Liu, C. L. Yu, C. X. Li, H. Y. Dai, H. F. Li, Y. L. Wang, and L. Jiang, "Uniform spread of high-speed drops on superhydrophobic surface by live-oligomeric surfactant jamming," Adv. Mater. **31**, 1904475 (2019).
[66]Y. S. Yu, L. Sun, X. F. Huang, and J. Z. Zhou, "Evaporation of ethanol/water mixture droplets on a pillar-like PDMS surface," Colloid Surf. A **574**, 215 (2019).
[67]Y. S. Yu, X. F. Huang, L. Sun, J. Z. Zhou, and A. Zhou, "Evaporation of ethanol/water mixture droplets on micro-patterned PDMS surfaces," Int. J. Heat Mass Transfer **144**, 118708 (2019).
[68]A. W. Adamson and A. P. Gast, *Physical Chemistry of Surfaces*, 6th ed. (John Wiley & Sons, Inc., New York, 1997).
[69]W. Kwieciński, T. Segers, S. van der Werf, A. van Houselt, D. Lohse, H. J. W. Zandvliet, and S. Kooij, "Evaporation of dilute sodium dodecyl sulfate droplets on a hydrophobic substrate," Langmuir **35**, 10453 (2019).
[70]R. Khalladi, O. Benhabiles, F. Bentahar, and N. Moulai-Mostefa, "Surfactant remediation of diesel fuel polluted soil," J. Hazard. Mater. **164**, 1179 (2009).

[71]T. Huhtamäki, X. Tian, J. T. Korhonen, and R. H. A. Ras, "Surface-wetting characterization using contact-angle measurements," Nat. Protoc. **13**, 1521 (2018).
[72]R. N. Wenzel, "Resistance of solid surfaces to wetting by water," Ind. Eng. Chem. **28**, 988 (1936).
[73]A. B. D. Cassie and S. Baxter, "Wettability of porous surfaces," Trans. Faraday Soc. **40**, 546 (1944).
[74]Q. S. Zheng, Y. Yu, and Z. H. Zhao, "Effects of hydraulic pressure on the stability and transition of wetting modes of superhydrophobic surfaces," Langmuir **21**, 12207 (2005).
[75]P. Attané, F. Girard, and V. Morin, "An energy balance approach of the dynamics of drop impact on a solid surface," Phys. Fluids **19**, 012101 (2007).
[76]Z. Xia, Y. Xiao, Z. Yang, L. Li, S. Wang, X. Liu, and Y. Tian, "Droplet impact on the super-hydrophobic surface with micro-pillar arrays fabricated by hybrid laser ablation and silanization process," Materials **12**, 765 (2019).
[77]T. Deng, K. K. Varanasi, M. Hsu, N. Bhate, C. Keimel, J. Stein, and M. Blohm, "Nonwetting of impinging droplets on textured surfaces," Appl. Phys. Lett. **94**, 133109 (2009).
[78]D. H. Kwon and S. J. Lee, "Impact and wetting behaviors of impinging droplets on textured surfaces," Appl. Phys. Lett. **100**, 171601 (2012).
[79]Y. Quan and L. Zhang, "Numerical and analytical study of the impinging and bouncing phenomena of droplets on superhydrophobic surfaces with microstructures," Langmuir **30**, 11640 (2014).